Chalcogenide Letters Vol. 22, No. 7, July 2025, p. 615 - 624

Boosting power efficiency in polycrystalline silicon solar cells: antimony selenide sputter coating with advanced optical, electrical, and thermal insights

R. M. Reddy [a], S. Chirag [b], T. Anu [c], A. R. Venkataramanan [d], S. Karthikeyan [e *], D. Palaniswamy [f], E. Venugopal Goud [a], N. Dineshbabu [g], T. Thirugnanasambandham [h]

[a] *Department of Mechanical Engineering, G.Pulla Reddy Engineering College, Kurnool, Andhrapradesh, India*
[b] *Department of Product Design, DLC state university of performing and visual arts, Rohtak, India*
[c] *Department of Multidisciplinary Engineering, The North Cap University, Gurugram, Haryana, India*
[d] *Department of Mechanical Engineering, Sona college of Technology, Salem, Tamil Nadu, India*
[e] *Department of Mechanical Engineering, Erode Sengunthar Engineering College, Perundurai, Tamil Nadu, India*
[f] *Department of Mechanical Engineering, Adithya Institute of Technology, Coimbatore, Tamil Nadu, India*
[g] *Department of Mechanical Engineering, Dhanalakshmi Srinivasan College of Engineering and Technology, Tamil Nadu, India*
[h] *Department of Mechanical Engineering, Saveetha School of Engineering, Saveetha Institute of Medical and Technical Sciences (SIMATS), Saveetha University, Tamilnadu, India*

Solar cells can transform light energy into electrical energy, possibly removing the need for fossil fuel energy resources. Reflection loss in solar cells is a factor contributing to diminished power conversion efficiency, which can be solved through using antireflective coatings on the cell surface. The present research primarily focuses on the development and application of antireflection coatings on the top surface of silicon solar cells. Sb_2Se_3 was deposited over multi-crystalline Si cells with different durations from 15 to 60 minutes. The influence of thin film Sb_2Se_3 coated cells was investigated through optical, current, voltage and thermal study. The ideal thickness of the Sb_2Se_3 coating was determined to be 1.336 µm for SB3 sample using FESEM. The lowest optical reflectance of 5.8% and highest absorbance of 93.4% was reached after 45 minutes of coating (SB3) across the 300 to 1200 nm wavelength band. The minimum electrical resistivity of a 45-minute coated Sb_2Se_3 sample was determined as 5.09×10^{-3} Ω-cm. The improved power conversion efficiency of Sb_2Se_3 coated solar cell under open sunlight setting was increased from 15.31 to 21.18% particularly for SB3 solar cell sample, which optimize maximum transfer of incident photons into the solar cell. From the observed results, it indicates that Sb_2Se_3 nanocoating has identified to be ideal antireflection coating material for polycrystalline silicon solar cells.

(Received April 4, 2025; Accepted July 11, 2025)

Keywords: Solar PV cells, Antimony selenide, Sputter deposition and Power conversion efficiency.

* Corresponding author: karthiksamynathan@gmail.com
https://doi.org/10.15251/CL.2025.227.615

1. Introduction

Solar power constitutes a notable progression in sustainable energy by capturing the sun's limitless radiation using technology such as PV panels. These panels, predominantly composed of semiconductor materials, transform the sunlight into electricity, rendering solar energy an economical and viable substitute for petroleum and coal. The increasing concern in solar power is motivated by its capacity to diminish greenhouse gases and effectively satisfy global power requirements [1]. Solar cells are essential for capturing the light energy and converting photons into electricity using the photovoltaic effect. The light absorbed energizes the electrons in semiconductor elements, resulting in the formation of electron-hole pairs to produce electricity [2]. Solar panels are predominantly consist of crystalline silicon, comprising either monocrystalline or polycrystalline silicon [3]. The technology for crystallized silicon PV cells is well-established and consistently maintains a significant position in the market. Recently, the performance of single-crystalline silicon cells has attained 22.3%, while polycrystalline cells have reached 18.75% [4]. However, silicon PV cells possess significant reflection, ranging from 30-35% for monocrystalline silicon and 25-30% for polycrystalline silicon at an effective wavelength of 600 nm. The main problem emerges from the electrical interaction of intrinsic semiconductor substances utilized in PV cells. Furthermore, the efficiency reductions due to reflected light in the glass of the panel (4% loss due to reflection) and degradation (36% reduction in transmittance) due to fine particles (dust and pollutants) requires immediate mitigation [5]. To sustain the steady progress and enhance present improvements, certain existing issues in the field of solar power must be rectified.

Using ARCs can substantially minimize reflectivity, resulting in the enhancement of power conversion of photovoltaic cells [6]. ARCs functions by the concept of destructive interference, whereas photons of various layers combined to negotiate specific wavelengths. The efficiency of an ARC is based upon its thickness, refractive index, and the angle of incident light. To achieve maximum effectiveness, the μ value of ARCs should present between air and silicon [7]. In this regard, ARCs on solar panels/modules enhance photon gathering by reducing reflection and provide shielding against erosive wear through enhanced transmittance.

To reduce reflective loss, several light control methods are being implemented, mono layer and dual layer coating with a change in μ value less than silicon cells [8]. The theoretical research and computations offer essential assistance for choosing ARCs with suitable materials along with thicknesses to improve PV cell efficiency. ARC simulations were utilized in several conditions to verify the highest possible efficiency [9]. The conventional method for decreasing surface reflection involves applying a low refractive index coating over the substrate. For anti-reflection coatings, highly transparent materials such as SiO_2, Si_3N_4, TiO_2, Al_2O_3, Ta_2O_5, and SiO_2–TiO_2 are used for c-Si solar cells [10]. Antireflective coatings were applied to solar cells using numerous physical deposition procedures, with a wide array of techniques utilized for coating in different situations. The broad spectrum of surface coating processes includes spin coating, PVD, CVD, thermo-spraying, electrodeposition [11].

Antimony selenide (Sb_2Se_3), a prospective ecologically harmless light-absorbing semiconductor material, has attracted significant attention due to its optoelectronic features. The Sb_2Se_3 thin film, as a binary substance, exhibits a strong light absorption coefficient (exceeding 10^5 cm^{-1}), an appropriate direct bandgap (~1.18 eV), and a modest hall mobility (around 10 cm^2/vs) [12]. Moreover, the availability, minimal toxic, reasonable cost, along with the ease manufacturing technique enhance the applicability of reliable PV cells in huge production. Significant advancements have been achieved in the performance of Sb_2Se_3-based PV panels in the last decade. However, maximum efficiency of Sb_2Se_3 thin-film PV cells is far below the mathematical calculation and substantially high than the widely investigated thin film $CuInGaSe_2$ (CIGS) PV panels [13].

Antimony selenide (Sb_2Se_3), an environmentally friendly and abundant material, has recently gained attention as a promising light-harvesting absorber for solar energy applications due to its favourable characteristics, including an appropriate bandgap, maximum absorption coefficient, satisfactory carrier mobility, basic binary phase composition, extraordinary long-term stability, and inherently harmless grain boundaries when properly oriented [14]. Significant advancements in Sb_2Se_3 PV cells have occurred over the past decade, with power conversion efficiency (PCE) rising

from 2.26% [15] to 9.2% [16] within a five-year span, hence receiving great attention recently. Despite this gain, the current optimum efficiency of Sb_2Se_3 PV cells is well below the theoretical prediction of approximately 32% [17], indicating substantial potential for performance enhancement.

In this research work, the antireflective Sb_2Se_3 has been applied on solar cells by sputter coating approach. The coating was performed under different coating intervals i.e. 15 min (SB1), 30 min (SB2), 45 min (SB3) and 60 min (SB4) mins coating time. Then, the Sb_2Se_3 coated cell was examined EDAX and XRD to confirm the presence of coating. The Sb_2Se_3 deposited cells were examined under the natural solar light. Additionally, absorbance, current, volage and reflection loss were evaluated for the deposited Sb_2Se_3.The entire coating process is provided in flow chart (Fig.1).

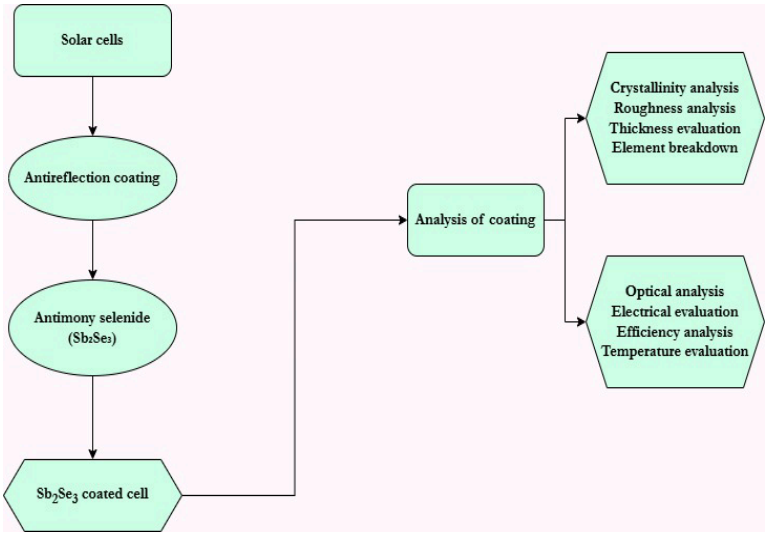

Fig. 1. Overview of Sb_2Se_3 coating process.

2. Methods of experimentation

2.1. Materials

The exceptionally pure antimony selenide has been bought from Sigma-Aldrich (India). The ethanol was purchased from Mahadev Chemicals in Chennai. The commercially available p-Si cells, sized 0.52 m × 0.38 m, was sourced from Vikram Solar (India).

2.2. Sputter deposition of Sb_2Se_3

Sb_2Se_3 films were applied onto the polycrystalline silicon solar cells through radio frequency (RF) sputtering. The Si cell substrate has been cleansed utilizing C_2H_5OH, C_3H_6O and de-ionization H_2O. The Sb_2Se_3 in the form of pellets were placed into surface plate for deposition. The target should be maintained at a distance of 50 mm distance from the silicon cell surface. Prior to applying ARC materials on silicon samples, a 5 min pre-sputter was executed. Subsequently, C_2H_5OH was employed to cleanse the coating specimen to eliminate contamination. The Si cell samples were subjected to the sputter procedure to create a Sb_2Se_3 antireflection coating with an optimal deposition duration of 15, 30, 45 and 60 mins.

2.3. Characterization techniques

Various approaches are employed to analyze the coating durability, adherence and performance of photovoltaic samples. The X-Ray diffraction (XRD) method is applied to identify the structural features of Sb_2Se_3 coated specimens. The AFM is utilized to analyze the coating quality and roughness of Sb_2Se_3 coated specimen with various duration on solar cells. The FESEM (MIRA 3, TESCAN) analysis performed for assessing the coating morphology and thickness of Sb_2Se_3 applied solar specimens. The element composition of the coating materials was identified using

EDAX, which verifies proper material deposition and layer adhesion. The UV spectroscopy was utilized to assess the absorption and reflectance, of bare and different durations of Sb_2Se_3 cell specimens. The four probe mechanism (SK012) is used for examining the electrical properties of uncoated and Sb_2Se_3 applied PV specimens. The current and voltage characteristics of PV cell specimens were assessed using a Keithley power module under open atmosphere circumstances. The IR thermal camera (Ti100 Series) gives images for analyzing the thermal response of both bare and different coated durations of Sb_2Se_3 specimens.

3. Results and findings

Fig. 2. illustrates the X- ray diffraction pattern of calcinated Sb_2Se_3 specimens at 900 °C. The observed peaks closely resemble the indexed configuration of Sb_2Se_3 (JCPDS file No.15-0861). The narrow peaks observed in the Sb_2Se_3 sample suggest a highest crystalline geometry. The acquired Miller indices (001), (002), (100), (101), (102), (110) and (111) are properly indexed with the Sb_2Se_3 structure. The presence of silicon has been confirmed by the peaks of crystalline. The positions of obtained peaks and the miller indices of Sb_2Se_3 coincide with the standard diffraction data.

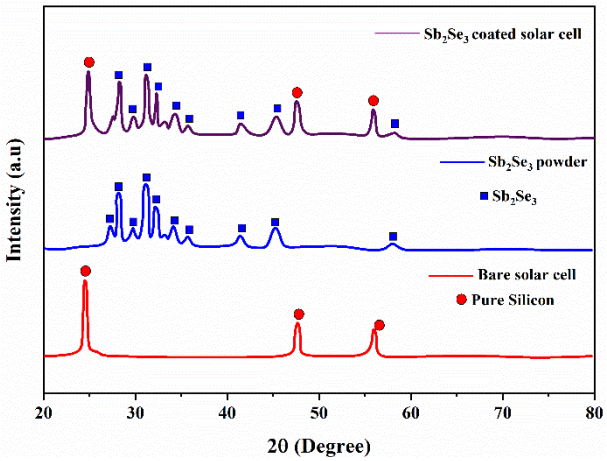

Fig. 2. X-ray diffraction evaluation of pure and Sb_2Se_3 deposited cells.

Fig. 3(a) and 3(b) shows FESEM images illustrating the coating morphology and cross section views of bare and SB3 deposited samples. Fig. 3(a) displays a compact, dense structure with partial pinhole morphology of Sb_2Se_3 coating. The layer thicknesses of the deposited Sb_2Se_3 cells (SB1 to SB4) were determined around 1.015 µm, 1.197 µm, 1.336 µm and 1.401 µm (Fig. 3). FESEM images clearly indicate that as the layers of Sb_2Se_3 deposition increase, the film thickness also increases, therefore enlarging the grain size. As seen, there exists a particle agglomeration for SB4 sample which reduces the PCE and optical properties of solar cells. Therefore, it is important to optimize the thickness and coating time.

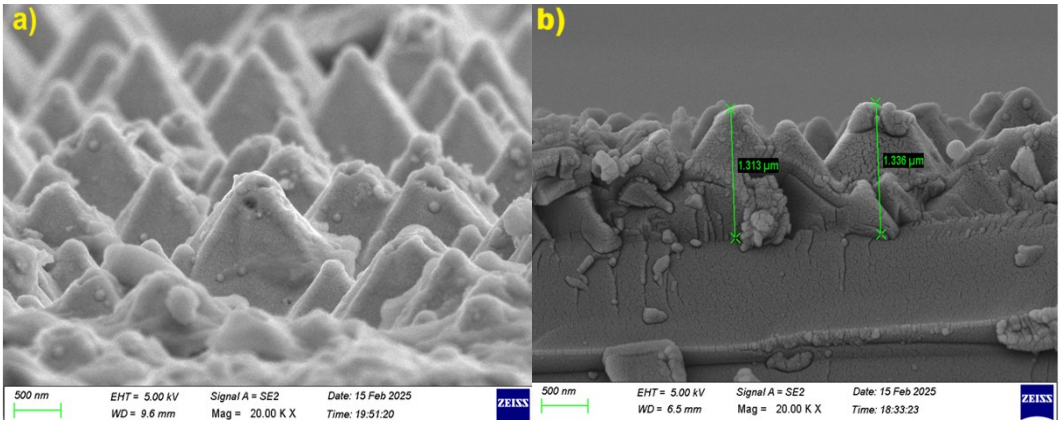

Fig. 3. (a) FESEM image and (b) Coating thickness of SB3 deposited cell.

The elements present in the coated silicon PV cell was verified using EDAX analysis. Fig. 3 illustrates the presence of multiple elements in the desirable surface coating of Sb_2Se_3, including Sb, Se, and Si. The large number of Si peaks were present due to the use of polycrystalline silicon as the photoactive material in PV cells.

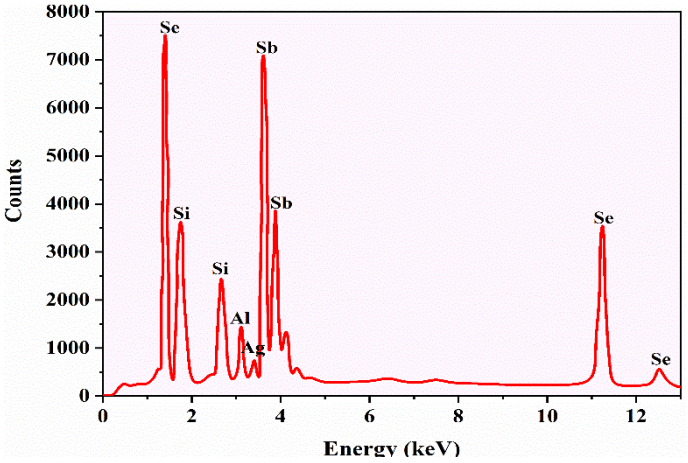

Fig. 3. EDAX analysis of Sb_2Se_3 coated Si solar cell.

The surface topography of Sb_2Se_3 applied on solar cells was examined with AFM. A 5 µm × 5 µm region was analyzed in a tapping method to determine the RMS value of Sb_2Se_3 coated solar cells. Fig. 4. depicts the 3D and 2D with depth profile of SB3 coated cell. Fig.4 shows clearly that the SB3 sample of Sb_2Se_3 exhibits an evenly coated surface.

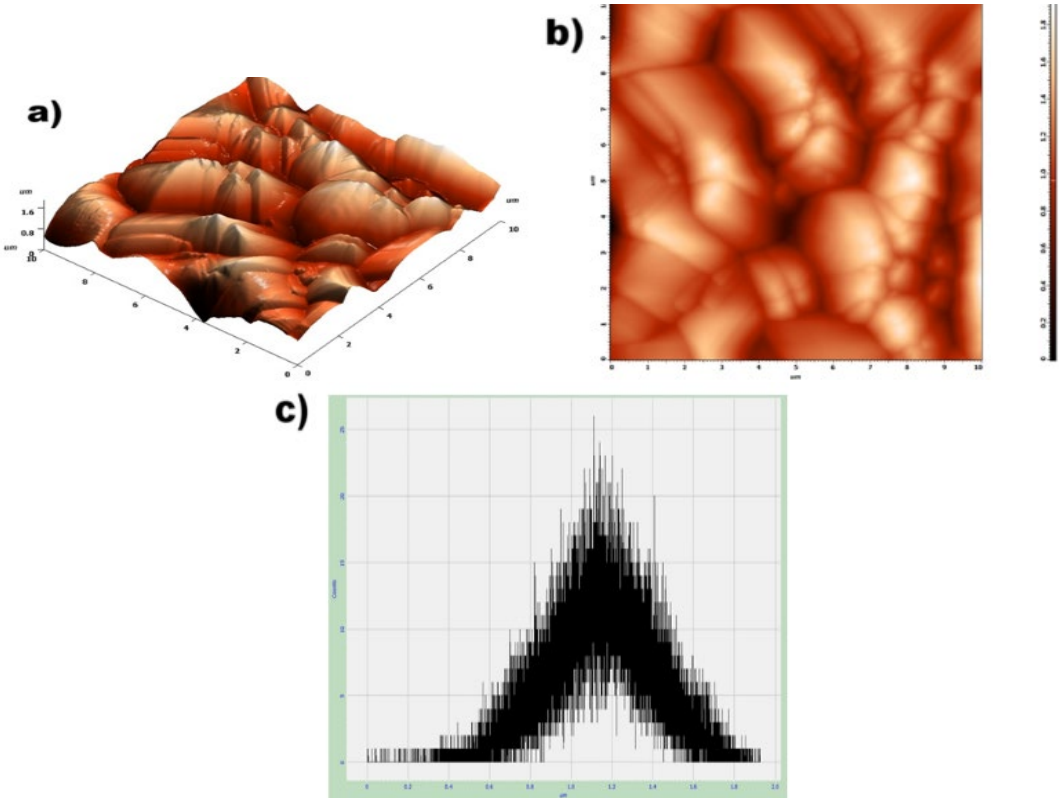

Fig. 4. AFM analysis of Sb_2Se_3 coated cells.

The RMS roughness of Sb_2Se_3 deposited on PV cells was assessed employing conventional software. The RMS roughness values for the SB1 to SB4 coating layers are 34 nm, 47 nm, 61 nm and 76 nm respectively. The consistency and smoothness of the surface are critical parameters for minimizing reflection losses, as a rough surface causes light scattering.

Fig. 5 demonstrates the absorption capability of Sb_2Se_3 deposited PV cells. The optical properties of Sb_2Se_3 and uncoated specimen was evaluated from 300 to 1200 nm range. As seen, the 45 mins (SB3) coating time achieves the highest absorption of 93.4% (Table 1) than the remaining specimen. The optical properties improve progressively with the coating time. The study illustrates that adjusting the ARC deposition time is essential for improving coating durability, minimizing reflectance, and enhancing absorption. Reflectance (R) findings for the bare cell, SB1, SB2, SB3, and SB4 photovoltaic samples are illustrated in Fig. 5(b). As observed, the SB3 coatings exhibit the lowest reflectance of 5.8%. The highest surface texture causes incoming light to become trapped in crevices, resulting in substantial interior reflections that reduces reflectance loss [18].

Table 1. Optical absorbance and reflectance spectra of bare cell and various Sb_2Se_3 coated photovoltaic cells.

Samples	Absorbance (%)	Reflectance (%)
Bare Cell	84.39	14.01
SB1	86.23	12.27
SB2	88.6	9.9
SB3	93.4	5.8
SB4	91.6	7.3

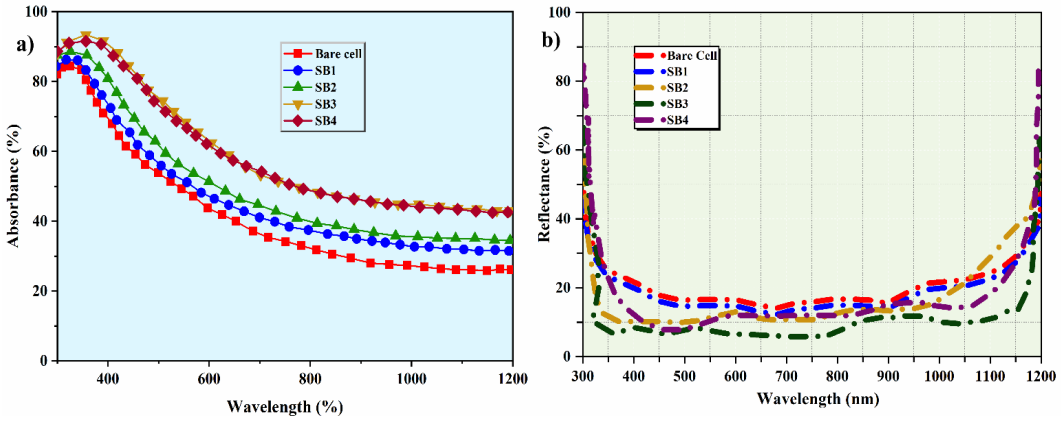

Fig. 5. (a) Absorbance and (b) reflectance of bare cell and Sb_2Se_3 deposited cells.

The electrical resistivity, carrier concentration, and hall mobility of Sb_2Se_3 deposited specimens were examined by a four-probe technique. The SB3 coating on the solar cell, applied for varying durations, demonstrates a low electrical resistance of 5.09×10^{-3} Ω cm (Fig. 6). The uncoated cell exhibits a maximum resistance of 10.32×10^{-3} Ω cm. The resistance decreases with increasing light transparency and carrier concentration, as demonstrated in Table 2. The SB3 coating attains the highest hall mobility (18.29 $cm^2\ V^{-1}s^{-1}$) and carrier concentration ($33.85\times10^{20}\ cm^{-3}$). The application of larger grain-sized materials with reduced grain boundaries markedly improves the rate of exciton generation and recombination. The exciton mobilization increases with the enhancement of photocurrent production and light intensity.

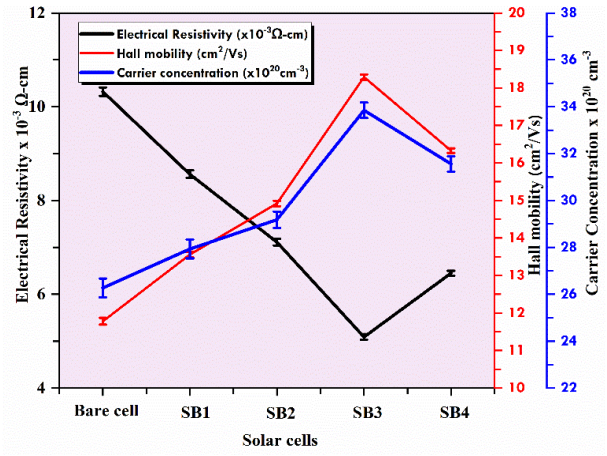

Fig. 6. Electrical features of bare and Sb_2Se_3 deposited cells.

Fig. 7 depicts the I-V characteristics of bare, SB1, SB2, SB3, and SN4 coated p-Si cells under direct sun rays. The voltage and current measurements were recorded and converted into an I-V profile, from which productivity may be assessed. The bare cell attains a power conversion efficiency (PCE) of 15.31%, the following parameters: Jsc = 35.76 mA/cm², Voc = 0.603 V, FF = 71%. The SB1, SB2, SB3 and SB4 are coated silicon solar cells have improved photocurrent output, achieving a power conversion efficiency (PCE) = 21.18% Jsc = 41.73 mA/cm², Voc = 0.651 V, and FF = 78% for SB3 sample (Table 3). A rise in Jsc and Voc leads to an enhancement in PCE from 15.31% to 21.18%. The improvement of fill factor leads to an increase in electricity generation. Further, the PCE declines for SB4 sample (20.03%), which may be due to the excessive particle agglomeration and increased grain size.

Table 2. Electrical properties of Sb_2Se_3 deposited cells.

Samples	Electrical Resistance (x 10^{-3} Ω-cm)	Hall mobility ($cm^2V^{-1}s^{-1}$)	Carrier concentration (x 10^{20} cm^{-3})
Bare Cell	10.32	11.78	26.27
SB1	8.56	13.56	27.93
SB2	7.11	14.92	29.18
SB3	5.09	18.29	33.85
SB4	6.45	16.33	31.56

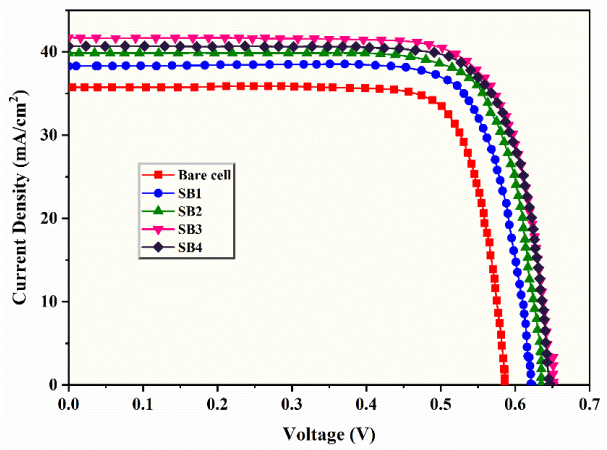

Fig. 7. Current-voltage properties of bare and coated cells under sunlight exposure.

Table 3. Photovoltaic current-voltage properties of pure cell and various Sb_2Se_3 coated cell under sunlight exposure.

Samples	J_{SC} (mA/cm^2)	V_{OC} (V)	FF (%)	PCE (%)
Bare Cell	35.76	0.603	71	15.31
SB1	38.27	0.623	73	17.40
SB2	39.85	0.635	75	18.97
SB3	41.73	0.651	78	21.18
SB4	40.68	0.648	76	20.03

Fig. 8 depicts the thermal analysis of (a) bare and (b) SB3 to assess the surface temperature of solar cells. The productivity of PV panels declines with increasing temperature. The infrared image technique is utilized for determining the operating temperature of different coated PV cells. The results indicate that SB3 sample demonstrates a lower temperature of 40.3 °C compared to bare (52.3°C) and other coated solar cells. The augmented light scattering increases the thermal transfer of solar cells, hence reducing the transparency of the anti-reflective coating. Thus, a reduced surface temperature enhances the efficiency of p-Si cells [19]. Consequently, it is clear that the Sb_2Se_3 layer served as an outstanding anti-reflective coating material for improving power conversion efficiency.

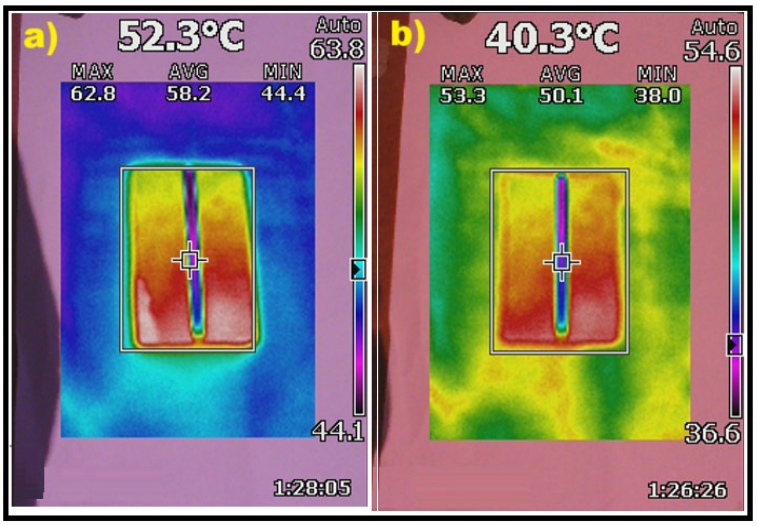

Fig. 8. IR thermal imaging (a) Bare and (b) SB3 coated cell under a sunlight source.

4. Conclusion

The Sb_2Se_3 ARC material was deposited onto the p-Si PV cell by sputter coating technique. The Miller indices (001), (002), (100), (101), (102), (110) and (111) are obtained from X-ray diffraction are closely correspond to Sb_2Se_3 crystal orientation. The surface roughness of various duration of Sb_2Se_3 coating such as SB1, SB2, SB3 and SB4 was 34 nm, 47 nm, 61 nm and 76 nm respectively. The FE-SEM evaluation reveals the cross-sectional thickness of 1.015 µm, 1.197 µm, 1.336 µm and 1.401 µm for the SB1, SB2, SB3 and SB4 coated cells, respectively. The Sb_2Se_3 coated solar cell demonstrates the highest absorbance of 93.4% and the lowest reflectance of 5.8% in comparison to bare cells and various ARCs applied on p-Si cells. The p-Si cells with a Sb_2Se_3 (SB3) anti-reflective coating exhibited superior PCE, achieving 21.18% at open sunlight conditions. The significant enhancement in the performance of Sb_2Se_3 applied on p-Si cells may be linked to the reorientation of the morphological and structural behavior of antireflective coating applied on solar cell substrate.

References

[1] M.O. Karaağaç, A. Ergün, O. Arslan, M. Kayfeci, Handbook of Thermal Management Systems. 2023, Elsevier. p. 541-556; https://doi.org/10.1016/B978-0-443-19017-9.00011-8

[2] S. Arya, P. Mahajan, Solar Cells: Types and Applications. 2023, Springer. p. 1-35; https://doi.org/10.1007/978-981-99-7333-0_1

[3] H. Soonmin, Hardani, P. Nandi, B.S. Mwankemwa, T.D. Malevu, M.I. Malik, Applied Sciences 13(4), 2023); https://doi.org/10.3390/app13042051

[4] M. Green, E. Dunlop, J. Hohl-Ebinger, M. Yoshita, N. Kopidakis, X. Hao, Progress in photovoltaics: research and applications 29(1), 2021); https://doi.org/10.1002/pip.3371

[5] M. Khalifa, M. Touil, K. Hammadi, I. Haddadi, A. Attyaoui, N. Meftah, F. Mannai, S. Aouida, H. Ezzaouia, Arabian Journal for Science and Engineering 2024).

[6] B. Swatowska, T. Stapinski, K. Drabczyk, P. Panek, Optica Applicata 41(2), 2011).

[7] Y.M. Adwan, M.M. Shabat, G. Zoppi, Journal of Applied Mathematics and Physics 11(5), 2023); https://doi.org/10.4236/jamp.2023.115092

[8] M. Huo, Y. Hu, Q. Xue, J. Huang, G. Xie, Molecules 28(5), 2023); https://doi.org/10.3390/molecules28052145

[9] N. Fakhri, M. Salay Naderi, S. Gholami Farkoush, S. SaeidNahaei, S.-N. Park, S.-B. Rhee, Energies 14(18), 2021); https://doi.org/10.3390/en14185944

[10] D.-S. Wuu, C.-C. Lin, C.-N. Chen, H.-H. Lee, J.-J. Huang, Thin Solid Films 584(2015); https://doi.org/10.1016/j.tsf.2015.01.042

[11] L. Dobrzański, M. Szindler, Journal of Achievements in Materials and Manufacturing engineering 59(1), 2013).

[12] W. Lian, R. Cao, G. Li, H. Cai, Z. Cai, R. Tang, C. Zhu, S. Yang, T. Chen, Advanced Science 9(9), 2022); https://doi.org/10.1002/advs.202105268

[13] W. Han, D. Gao, R. Tang, Y. Ma, C. Jiang, G. Li, T. Chen, C. Zhu, Solar RRL 5(3), 2021); https://doi.org/10.1002/solr.202000750

[14] A. Mavlonov, T. Razykov, F. Raziq, J. Gan, J. Chantana, Y. Kawano, T. Nishimura, H. Wei, A. Zakutayev, T. Minemoto, Solar Energy 201(2020); https://doi.org/10.1016/j.solener.2020.03.009

[15] Y. Zhou, M. Leng, Z. Xia, J. Zhong, H. Song, X. Liu, B. Yang, J. Zhang, J. Chen, K. Zhou, Advanced energy materials 4(8), 2014); https://doi.org/10.1002/aenm.201301846

[16] Z. Li, X. Liang, G. Li, H. Liu, H. Zhang, J. Guo, J. Chen, K. Shen, X. San, W. Yu, Nature communications 10(1), 2019); https://doi.org/10.1038/s41467-018-07903-6

[17] W. Shockley, H. Queisser, Renewable energy. 2018, Routledge. p. Vol2_35-Vol2_54; https://doi.org/10.4324/9781315793245-44

[18] W. Wang, L. Qi, Advanced Functional Materials 29(25), 2019); https://doi.org/10.1002/adfm.201807275

[19] A. Alshammari, E. Almatrafi, M. Rady, Solar Energy 273(2024); https://doi.org/10.1016/j.solener.2024.112545